

**NASA
Technical
Paper
1942**

**AVRADCOM
Technical
Report
81-C-7**

December 1981

NASA
TP
1942
c.1



Gas Turbine Ceramic-Coated-Vane Concept With Convection-Cooled Porous Metal Core

Albert F. Kascak,
Curt H. Liebert,
Robert F. Handschuh,
and Lawrence P. Ludwig

LOAN COPY: RETURN TO
AFWL TECHNICAL LIBRARY
KIRTLAND AFB, N. M.

NASA

**NASA
Technical
Paper
1942**

**AVRADCOM
Technical
Report
81-C-7**

1981

TECH LIBRARY KAFB, NM



0067699

Gas Turbine Ceramic-Coated-Vane Concept With Convection-Cooled Porous Metal Core

Albert F. Kascak

Propulsion Laboratory

AVRADCOM Research and Technology Laboratories

Lewis Research Center

Cleveland, Ohio

Curt H. Liebert,
Robert F. Handschuh,
and Lawrence P. Ludwig

Lewis Research Center

Cleveland, Ohio



National Aeronautics
and Space Administration

Scientific and Technical
Information Branch

Summary

Analysis and flow experiments on a ceramic-coated-porous-metal vane concept indicated the feasibility, from a heat transfer standpoint, of operating in a high-temperature (1644 K; 2500° F) gas turbine cascade facility. The heat transfer and pressure drop calculations provide a basis for selecting the ceramic layer thickness (to 2.03 mm; 0.08 in.), which was found to be the dominant factor in the overall heat transfer coefficient. Also an approximate analysis of the heat transfer in the vane trailing edge revealed that with trailing-edge ejection the ceramic thickness could be reduced to 0.254 millimeter (0.01 in.) in this portion of the vane.

Introduction

Continuing demand for improved performance (thrust and efficiency) drives gas turbine designs toward ever increasing temperatures in the turbine assemblies, which are composed of metallic components and are cooled in order to meet operating life goals. Therefore an increase in turbine gas temperature has an associated increase in cooling airflow requirement, which brings about a point of diminishing return on performance improvement because of the penalty associated with bleeding off air for cooling.

As compared with cooling large engines, small engines have additional problems of larger penalty associated with bleeding air and with incorporation of cooling passages and holes in small vanes and other components. For these reasons small engines generally employ less cooling technology than large engines, and by necessity operate at lower temperatures.

In an effort to find solutions to these small-engine cooling problems, considerable work has been expended in developing monolithic ceramic components that can operate uncooled; in this regard, references 1 to 3 are a few examples of the extensive work in this area. The inherent low tensile strength and brittleness of monolithic ceramics makes application difficult.

Another approach to obtain high-temperature components without a large cooling penalty has been applied by reference 4 to end walls over turbine blade tips. This approach makes use of ceramic sprayed

onto a porous metal layer. The low modulus of this porous metal layer acts to mitigate the thermal strain differences between the ceramic and the metal base structure to which the porous metal is brazed. The porous metal provides an excellent bonding surface for the sprayed ceramic layer, and excellent mechanical and thermal shock resistance are reported (ref. 5).

This ceramic-coated-porous-metal concept may prove to be useful for other static components such as the vane concepts described in reference 6. One version of this concept is composed of a plasma-sprayed ceramic coating applied over an airfoil-shaped porous metal core. The ceramic coating acts as a thermal barrier, and a small amount of cooling air flows spanwise through the porous metal core.

The objectives of this work are to establish the feasibility of this vane concept by measuring the pressure drop in the porous metal that would be used in a vane core and by formulating mathematical models for the prediction of temperatures and cooling mass flow. Three different gases (air, argon, and helium) were used in the flow studies on porous metals, and mass flow rates were recorded as a function of pressure drop across the porous metal specimen. Generally the flow rates were in a very low Reynolds number regime. From the flow data an average hydraulic diameter and associated friction factor were calculated. These data, in conjunction with heat transfer analysis, were used to judge the feasibility of the vane concept.

Background and Analysis

Vane Concept

The basic vane concept, which is shown in figure 1, consists of a porous metal airfoil shape that is oversprayed with a ceramic coating. Cooling airflow is in a radial direction, that is, normal to the axial flow of the turbine gas. And heat conduction is through the ceramic coating, which acts as a thermal barrier, into the porous metal region. This ceramic/porous metal concept is considered suitable for limited-life engines, in which plugging of the porous metal would not be a problem. A nonplugging concept for long life (ref. 6) was not evaluated in this study.

The vane core, which is a 75-percent-porosity metal, is shown in figure 2 prior to ceramic coating. The span of the test vane was determined by heat transfer and flow analysis (see following sections) and was selected to be 25.4 millimeters (1.0 in.). The airfoil core cross-sectional area (normal to the cooling airflow direction) was 387 square millimeters (0.6 in²); this cross-sectional area has a perimeter of 127 millimeters (5 in.). The vane core was fabricated (by electron discharge machining) from a slab of NiCrFeMo alloy porous metal. A scanning electron photomicrograph (fig. 3) shows the surface after fabrication. Internal surface area measured by a gas absorption method was 0.8 m²/g (4345 ft²/lbm).

A ceramic coating of ZrO₂ was plasma sprayed onto the porous metal airfoil shape and conceptually covered the entire airfoil with a constant-thickness coating except at the trailing edge, which was left uncovered for trailing-edge ejection (fig. 1). The procedure for coating the porous metal core consisted of (1) grit-blasting with pure aluminum oxide particles, (2) plasma-spraying a bond coating of Ni-16Cr-6Al-0.64Y on the porous metal core, and (3) plasma-spraying a ceramic coating of 8-weight-percent-yttria-stabilized zirconia (ZrO₂) onto the bond coating.

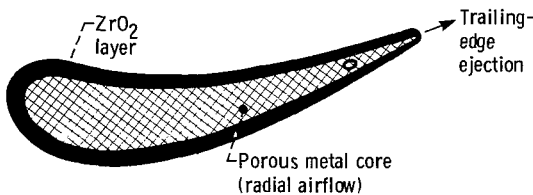
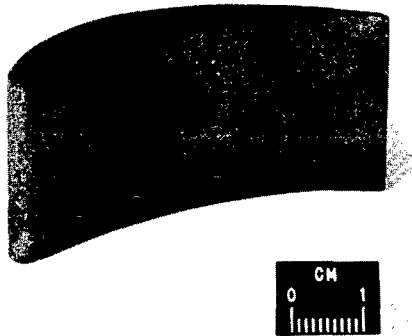


Figure 1. - Ceramic-coated porous metal vane concept.



C-80-6735

Figure 2. - Vane core made from porous metal.

Trailing-edge ejection is needed in order to maintain acceptable temperature levels in this thin portion of the vane. In this regard the thicker section of the vane is visualized to have predominately spanwise flow and the trailing edge to have axial flow. This flow is established in the vane by a hole in the core that feeds cooling air to the trailing edge (fig. 4).

Vane Heat Transfer Analysis

A simplified mathematical model that was used to formulate the heat transfer analysis is shown in figure 5. The model is based on the following assumptions:

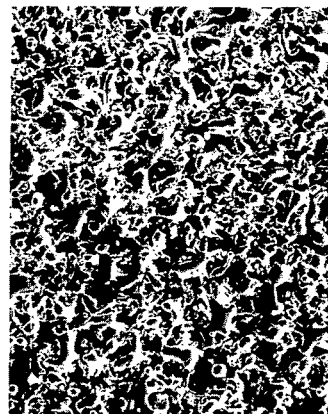


Figure 3. - Scanning electron photomicrograph of porous metal surface (after electric discharge machining).

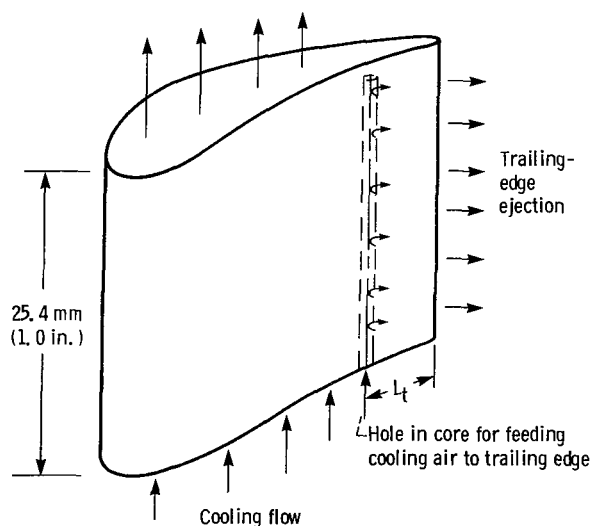
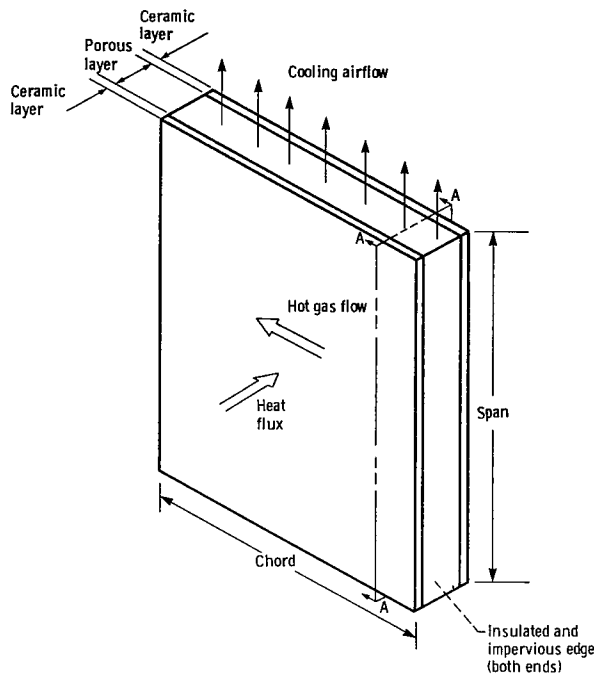
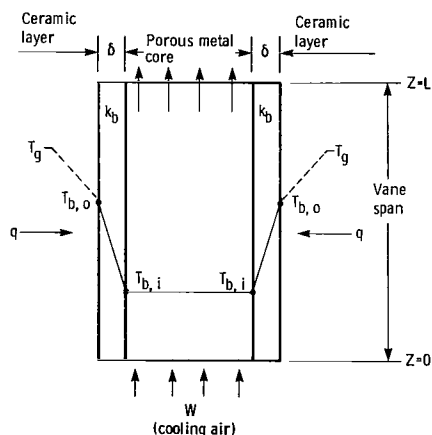


Figure 4. - Sketch of test vane core showing location of trailing-edge cooling hole.



(a) Simplified vane.



(b) Section A - A - A.

Figure 5. - Vane mathematical model.

(1) The heat flux through the ceramic layer is one dimensional. (Ceramic thermal conductivity values were obtained from ref. 7.)

(2) The cooling airflow Reynolds number is low; therefore the porous metal temperature is not significantly greater than the cooling air temperatures and the two temperatures can be considered equal (refs. 8 and 9).

(3) The cooling airflow through the porous metal core is one dimensional, and a thermal gradient in the porous metal exists only in the cooling airflow direction.

(4) A flat-plate model was used to calculate the hot-gas-to-surface heat transfer coefficient, and this coefficient was assumed to be constant and applicable to the entire vane surface. Reference 10 shows that the flat-plate coefficient, based on the initial hot-gas inlet conditions to its vanes, is conservative (larger than the actual coefficient).

This fourth assumption regarding the hot-gas film coefficient can be further justified (see results section) on the basis that the conductivity of the hot-gas film is generally larger than the conductivity of the ceramic layer; therefore the solution is not sensitive to the accuracy of the hot-gas film coefficient. Assumed test conditions used to predict vane core operating temperature are given in table I.

With reference to figure 5(b), the heat flux equation for the gradient through the hot-gas film and ceramic layer is

$$q = h_g(T_g - T_{bo}) = \frac{k_b}{\delta}(T_{bo} - T_{bi})$$

$$= h_{eff}(T_g - T_{bi}) \quad (1)$$

in which, q is the heat flux, h_g is the hot-gas film coefficient, k_b is the conductivity of the ceramic layer, and h_{eff} is the overall heat transfer coefficient. This heat flux is conducted into the porous metal and then into the cooling air; the following holds:

$$qs = Wc_p \frac{dT}{dZ} \quad (2)$$

in which s is the perimeter of the vane airfoil shape, W is the mass flow of the cooling air, and c_p is the specific heat.

TABLE I.—OPERATING CONDITIONS AND FLUID

PROPERTY DATA

	Turbine hot gas	Cooling air
Entrance temperature, K (°F)	1644 (2500)	294 (70)
Inlet pressure, atm	10	10
Specific heat, c_p , J/g K (Btu/lbm °F)	1.046 (0.25)	1.046 (0.25)
Kinematic viscosity, γ , cm ² /sec (in ² /sec)	0.196 (0.0304)	0.0149 (0.0023)

Equations (1) and (2) can be combined to give

$$(T_g - T) = \frac{Wc_p}{h_{eff}s} \frac{dT}{dZ} \quad (3)$$

where h_{eff} is the overall heat transfer coefficient and Z is the vane span. Integration of equation (3) and application of the boundary condition of $T = T_{co}$ at $Z = 0$ result in the following relationship:

$$W = \frac{h_{eff}sL}{c_p} \frac{1}{\ln(T_g - T_{co})/(T_g - T_{ci})} \quad (4)$$

in which T_{co} is the entrance cooling air temperature and T_{ci} is its exit cooling air temperature at $Z = L$. Equation (4) can be used to predict the maximum vane core temperature T_{ci} as a function of cooling air mass flow.

Vane Flow Analysis

The flow in the porous metal was modeled like pipe flow; and since the Reynolds number was assumed to be low, the friction factor for laminar pipe flow was used. That is,

$$F = \frac{64}{Re} = \frac{64\mu}{\rho V d_h} \quad (5)$$

where d_h is the hydraulic diameter for the porosity of the metal core, ρ is the fluid density, V is the average velocity in the pores, and μ is the fluid viscosity. Also the following applies:

$$F = - \frac{d_h}{\frac{1}{2}\rho V^2} \frac{dP}{dZ} \quad (6)$$

in which dP/dZ is the pressure gradient along the span. Equating (5) and (6) gives

$$\frac{dP}{dZ} = - \frac{32\mu(\rho V)}{\rho(d_h)^2} \quad (7)$$

In which $(d_h)^2/32$ corresponds to the permeability coefficient of the Darcy equation as given in reference 11. It is convenient to make the following substitutions into equation (7):

$$\rho V = W/\epsilon A$$

ϵ is porosity, A is the flow area

$$dZ = Wc_p dT/h_{eff}s(T_g - T)$$

(see eq. (3))

$$\gamma = \mu_{co} \sqrt{\frac{T}{T_{co}}} / \rho_{co} \left(\frac{P}{P_{co}} \right) \left(\frac{T}{T_{co}} \right)^{-1}$$

(variable property relationship in which γ is the kinematic viscosity)

$$W = \frac{h_{eff}sL}{c_p} \frac{1}{\ln(T_g - T_{co})/(T_g - T_{ci})}$$

and the result after integration is

$$\left(\frac{P}{P_{co}} \right)^2 = 1 - \left(\frac{64\gamma_0 h_{eff}sL^2}{\epsilon A d_h^2 P_{co} c_p} \right) \times \left\{ \frac{I(X_{ci}) - I(X_{co})}{X_{co}^{3/2} [\ln(1 - X_{co})/(1 - X_{ci})]^2} \right\} \quad (8)$$

in which

$$I(X) = \int \frac{X^{3/2} dX}{1 - X} = -\frac{2}{3} X^{3/2} - 2X^{1/2} + \ln \left(\frac{1 + X^{1/2}}{1 - X^{1/2}} \right)$$

and

$$X = \frac{T}{T_g}$$

With reference to equation (8), the hydraulic diameter d_h is the only unknown, and this was determined in a series of flow tests (see following sections) on the particular core material used to construct the vane.

Apparatus and Procedure

Experiments on Flow Through Porous Metals

A schematic of the flow test rig used to measure pressure drop across the porous metal specimen is

shown in figure 6. This pressure drop was measured by a differential pressure transducer. Upstream and downstream static pressures were measured by gages connected to wall taps; these pressure gages also provided a check on the differential pressure transducer. The static pressure at the inlet to the rotometer was also measured by a pressure gage and provided the basis for flow rate calculations. Upstream and downstream gas temperatures were measured by thermocouples. The porous metal specimen was the same NiCrFeMo metal alloy of 75 percent porosity used to construct the vane core. The specimen was cylindrical in shape, 20.02 millimeters (0.788 in.) long and 19.05 millimeters (0.75 in.) in diameter.

Typical test procedure for each test point consisted of setting a desired pressure level at the inlet to the rotometer; this pressure level corresponded to one of the two pressure levels, 23.9 and 37.8 N/cm² abs (34.7 and 54.7 psia), used in calibrating the rotometer. During the test the upstream and downstream temperatures were monitored, and these did not vary by more than a few degrees from room temperature 293 K (68° F). Essentially a range of pressure differentials across the porous metal specimen was established by regulating of upstream and downstream valves, and data were taken after flow equilibrium was established. Pressure differential and mass flow were measured for three different gases (air, argon, and helium). The measured mass flow together with the measured pressure differential across the specimen was used to construct curves of flow as a function of pressure differential. From these data an average hydraulic

diameter was determined; this calculation, being based on the assumption of viscous-dominated flow, made use of the relationship that the flow friction factor F was equal to $64/Re$.

Results and Discussion

Flow Through Porous Media

Flow tests were made as described in the preceding section. These test data, shown in figure 7 for three different gases (air, argon, and helium), allow calculation of the hydraulic diameter by use of equation (7). The calculated hydraulic diameter from all the data in figure 7 is shown in figure 8, from which the average calculated hydraulic diameter has been determined to be 0.000016 meter (0.000051 ft). This average value of hydraulic diameter was used in calculating pressure drop and heat transfer in the test vane core.

Vane Heat Transfer

Equation (1) was used to get a measure of the relative effectiveness of the ceramic coating as a thermal barrier. In this calculation the ceramic thermal conductivity was taken as a constant with temperature. Data in references 7 and 12 suggest that the variation of the thermal conductivity is not significant up to temperatures in the range 1360 K (2500° F) (k_b is approximately 0.006 W/cm K, ref. 7). With reference to figure 9, as the ceramic thickness approaches zero, the indicated film

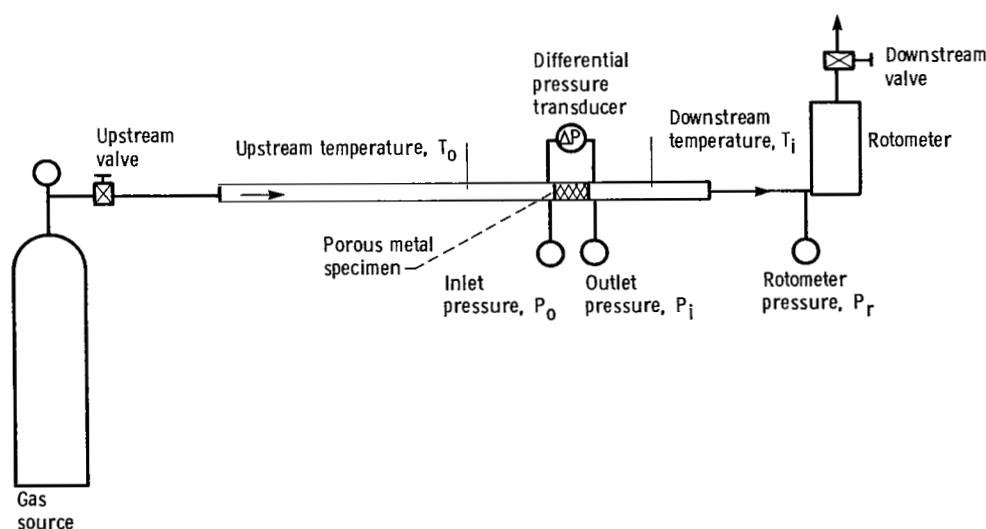


Figure 6. - Schematic of apparatus used to measure pressure drop as a function of mass flow.

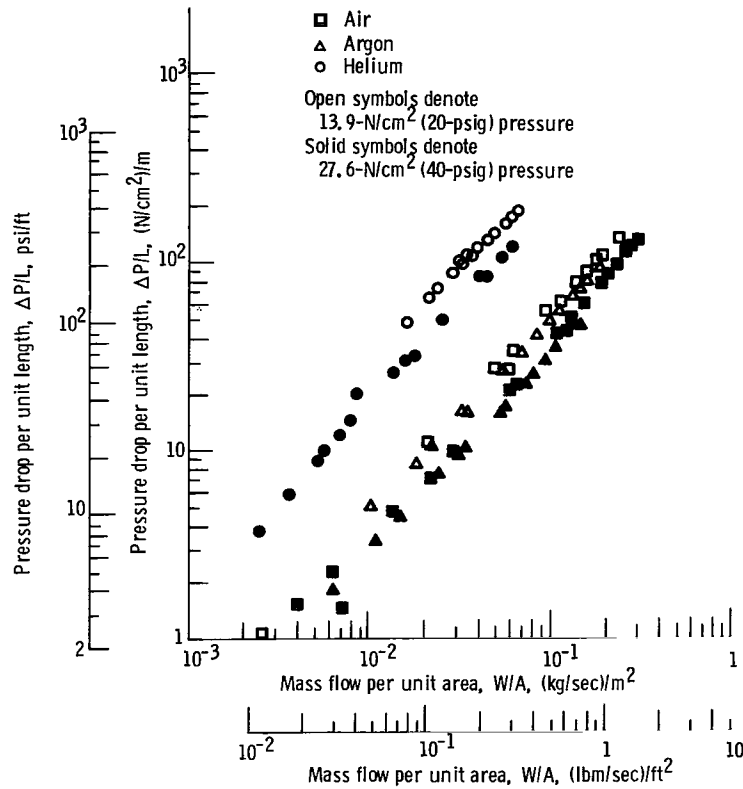


Figure 7. - Pressure gradient as function of gas flow through porous metal (75 percent porosity).

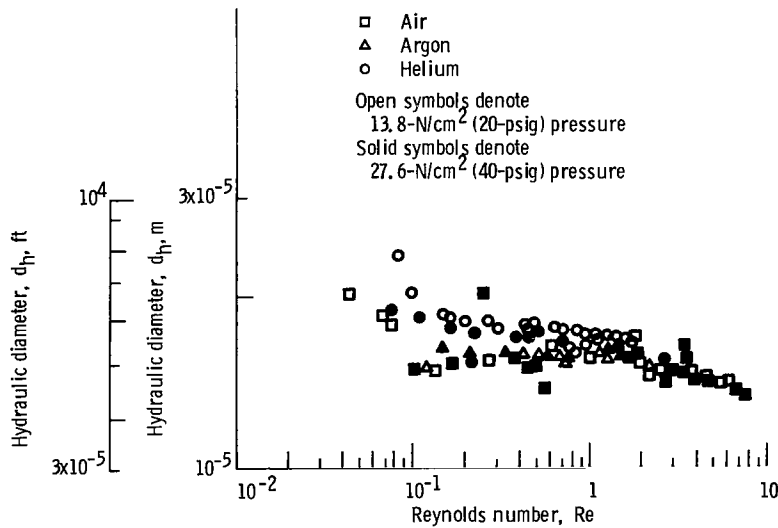


Figure 8. - Calculated hydraulic diameter as function of Reynolds number for gas flow through porous metal (75 percent porosity).

coefficient approaches 0.08 $\text{W/cm}^2 \text{ K}$ (0.00086 $\text{Btu/in}^2 \text{ sec } ^\circ\text{F}$); this is really a measure of the hot-gas film coefficient since the ceramic contribution is

zero. As the ceramic layer thickens, the contribution of the hot-gas film coefficient is decreased, and above 1.02-millimeter (0.04-in.) layer thickness the

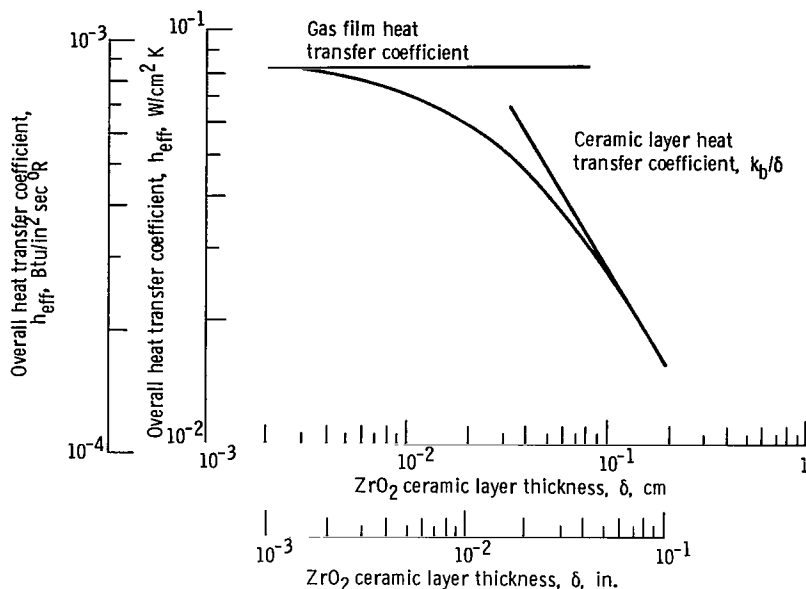


Figure 9. - Effective heat transfer coefficient as function of ceramic layer thickness.

overall heat transfer is markedly influenced by the ceramic thickness.

Equation (4) provides the mass flow needed to maintain given levels of exit air temperature from the test vane core; the results of the analysis are shown in figure 10. With reference to figure 10, as the thickness of the ceramic layer is increased, the cooling flow required for any given exit air temperature decreases significantly. (This is a result of the good thermal barrier characteristic of the ceramic layer.) From oxidation considerations, 1144 K (1600° F) was selected as a maximum porous metal temperature (cooling flow exit temperature), and the curves show the cooling flow required for that temperature is about 0.003 kg/sec (0.006 lbm/sec) for the test vane with a 1.02-millimeters (0.04-in.) thick layer of ZrO₂.

Equation (8) permits determination of the pressure drop through the test vane; the results of the analysis are shown in figure 11. For the example of a core with a ceramic coating of 1.02 millimeters (0.04 in.) the pressure drop is about 26 N/cm² (38 psi).

Equation (8) can be expressed in a manner more convenient for design purposes, as shown in figure 12, in which the pressure drop of the cooling flow is plotted as a function of span length for three different cooling flow exit temperatures T_{ci} . From this figure it is quite apparent that spans greater than 3.5 centimeters (1.38 in.) are not practical because of the rapidly increasing pressure drop; a 2.5-centimeter (1.00-in.) span was selected for experimental study since the pressure drop for this span length is reasonable.

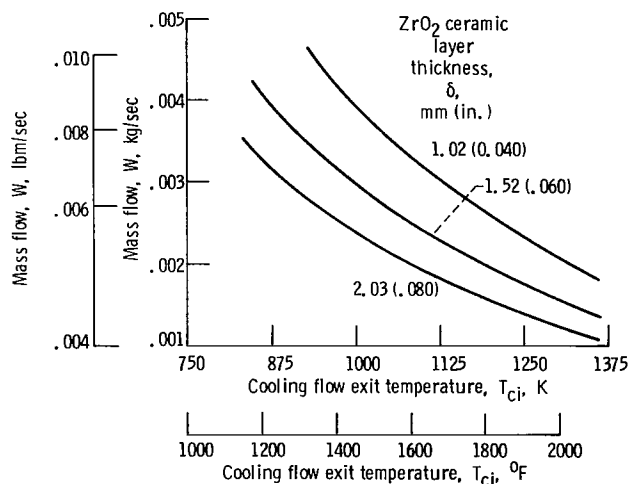


Figure 10. - Vane cooling flow requirement as function of ceramic layer thickness.

Trailing-Edge Ejection

The mathematical model of figure 5 applied in the preceding section predicts the temperatures for a vane thickness of about 6.35 millimeters (0.25 in.). In those sections of the vane where the core is thinner, such as at the trailing edge, the model will underestimate the temperature. This trailing-edge temperature problem is handled by trailing-edge ejection of the cooling flow. In order to estimate the ceramic thickness needed to protect the rather thin (1.27 mm; 0.05 in.) porous metal of the trailing edge,

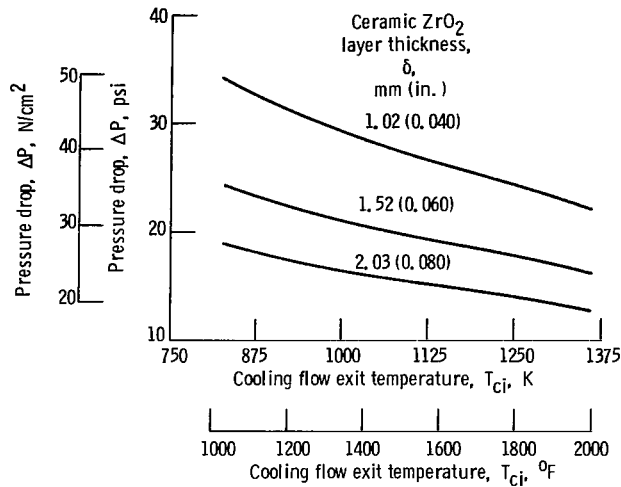


Figure 11. - Pressure drop as function of porous metal exit core (cooling flow exit) temperature.

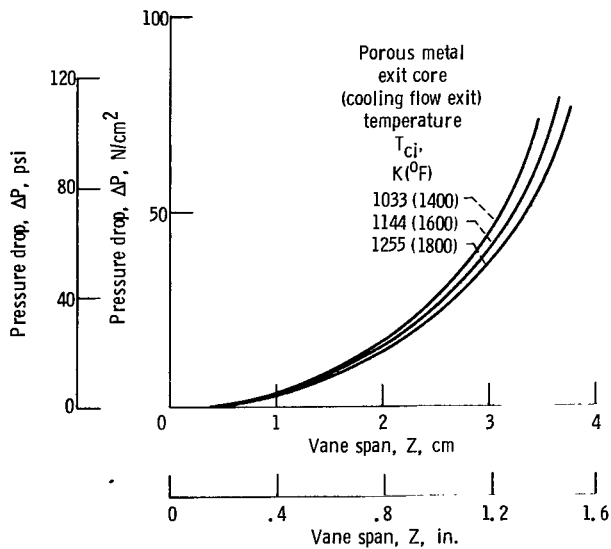


Figure 12. - Pressure drop in vane span as function of span length for three exit cooling gas temperatures in porous metal.

it was modeled in a fashion similar to that shown in figure 5. The differences were that the cooling flow length was 6.35 millimeters (0.25 in.) and that the entrance cooling flow temperature was assumed to be 294 K (70° F) since the source was a spanwise hole (fig. 4). The results of the analysis are shown in figures 13 to 15.

The cooling flow required to maintain the indicated cooling flow exit temperatures on the ordinate are shown in figure 13 for 0.25, 0.51, 0.76, and 1.02 millimeters (0.01, 0.02, 0.03, and 0.04 in.) thicknesses of ceramic. For example, if 1144 K (1600° F) is selected as the maximum allowable

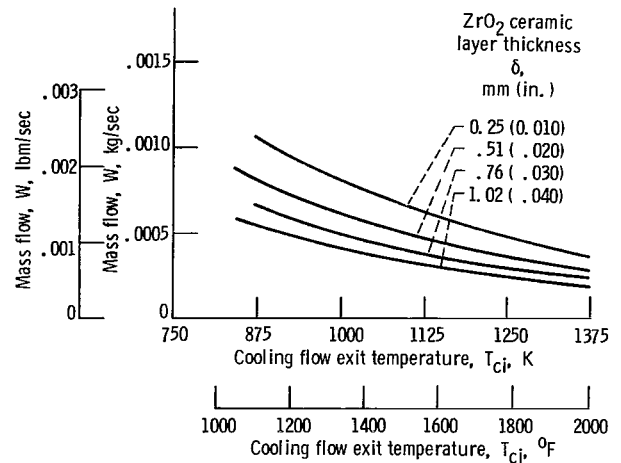


Figure 13. - Cooling mass flow in trailing edge (trailing-edge ejection) as function of cooling flow exit temperature for various ceramic thicknesses.

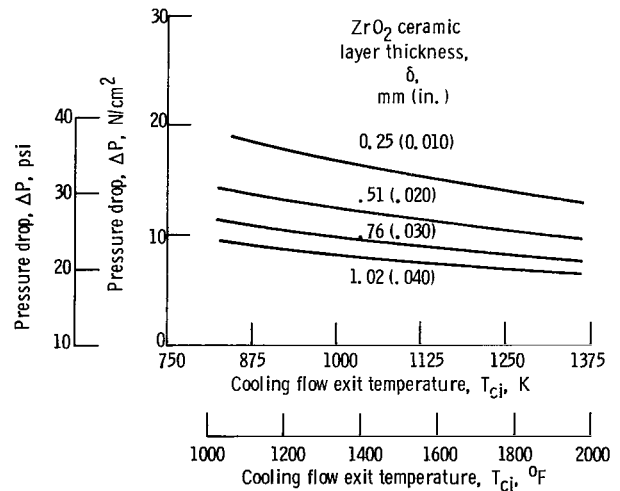


Figure 14. - Pressure drop in trailing edge (trailing-edge ejection) as function of cooling flow exit temperature for various ceramic layer thicknesses.

cooling flow exit temperature, the required cooling weight flow is 0.0005 kg/sec (0.0011 lbm/sec) when the ceramic thickness is 0.25 millimeter (0.01 in.). And in figure 14 the pressure drop for trailing-edge ejection is displayed as a function of cooling flow exit temperature. For example, for a rather thin ceramic thickness of 0.25 millimeter (0.01 in.) and an allowable exit temperature of 1144 K (1600° F), the pressure drop is about 16 N/cm² (23 psi); this is an acceptable gradient.

Finally in figure 15 the pressure drop is plotted as a function of cooling flow source (hole) distance L_t from the trailing edge (see fig. 4). The data indicated

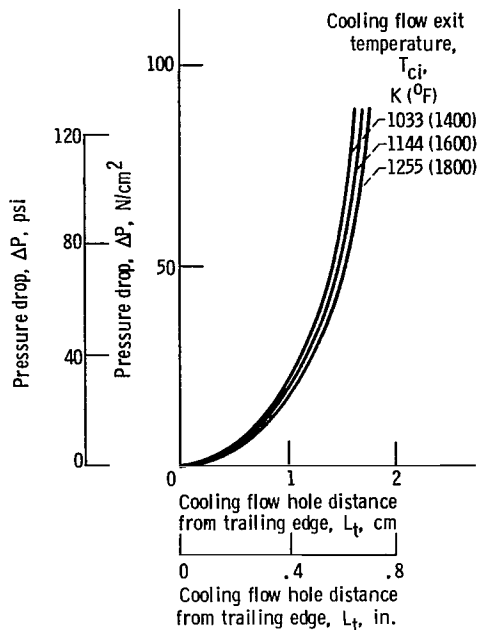


Figure 15. - Pressure drop in cooling airflow in trailing-edge portion as function of cooling flow distance from trailing edge for three cooling flow exit temperatures.

that distances greater than 1.5 centimeters (0.6 in.) are not practical; a distance of 0.63 centimeter (0.25 in.) was selected since the calculated pressure drop was acceptable for this distance.

Concluding Remarks

The pressure drop of the required cooling flow through the porous core of the vane is an important engine design consideration since exit pressure level determines the location at which the flow can be returned to the engine flow path or determines if the flow can be used for additional cooling. Therefore minimum pressure drops are desired. In this regard, selection of a lower density core material such as one of 0.85 porosity will reduce the pressure drop by a factor of about 5. However, in changing to 0.85 porosity the metal core thermal conductivity decreases and the thermal gradients normal to the vane core may start to become significant, according to Wong and Bybbs.

The pressure drop calculations for the 0.75 porous core indicate feasibility for use in high-pressure engines, in which pressure drops of 20.7 to 27.6

N/cm^2 (30 to 40 psi) are acceptable. Further for small engines the vane spans are often much less than 1 inch; therefore the pressure drop tends to become less significant and thinner ceramic layer thicknesses (with associated higher cooling flows) may be acceptable. The vane trailing edge presents a special problem since spanwise flow alone will not provide sufficient cooling. Therefore trailing-edge ejection was used to cool the rather thin layer of porous metal in this portion of the blade. In this regard the mathematical model used does not accurately model the two-dimensional flow in the region of the feed hole for trailing-edge cooling. However, it was judged that this simplification was not critical for feasibility analysis purposes.

Summary of Results

A new vane concept composed of a porous metal core oversprayed with an yttria-stabilized zirconia (ZrO_2) ceramic layer was proposed for high-temperature turbines. As a check on feasibility, experiments were made on cooling flow pressure drop through the porous metal core material as a function of mass flow. These experiments provided a measure of the hydraulic diameter of the core porosity based on an analogy to the friction factor in laminar pipe flow; the low Reynolds number of the flow seems to justify this assumption. A heat transfer analysis of a particular vane geometry provided the required cooling flows as a function of ceramic layer thickness needed to maintain cooling flow exit temperature within given limits set by the oxidation rate of the porous metal. And finally flow analysis (based on prior testing) provided the pressure drop associated with the cooling flow. These flow tests and vane heat transfer analysis indicated the following:

1. The ceramic-coated-porous-metal vane concept is feasible from a porous metal core temperature and cooling flow standpoint.
2. The overall heat transfer coefficient is markedly affected by the ceramic layer thickness.
3. With trailing-edge ejection the porous metal core temperature in the trailing edge can be kept within design limits by acceptable cooling mass flows and pressure drops.

Lewis Research Center
National Aeronautics and Space Administration
Cleveland, Ohio, April 27, 1981

Appendix—Symbols

A	flow area, cross-sectional area of vane airfoil shape	γ	kinematic viscosity
c_p	specific heat	δ	thickness
d_h	hydraulic diameter	ϵ	porosity
F	friction factor	μ	viscosity
g	acceleration due to gravity	ρ	density
h	heat transfer coefficient	Subscripts:	
k	thermal conductivity	bi	ceramic thermal barrier inside
L	length	bo	ceramic thermal barrier outside
P	pressure	ci	cooling air exit
ΔP	pressure drop	co	cooling air entrance
q	heat flux	e	equivalent overall
Re	Reynolds number	eff	effective
s	perimeter of airfoil shape	g	turbine hot gas
T	temperature	p	porous metal
V	velocity	r	rotometer
W	mass flow	t	trailing edge
Z	vane span		

References

1. Hudson Michael S.; Janovicz, Michael A.; and Rockwood Franklin A.: Ceramic Applications in Turbine Engines. (EDR-10156, Detroit Diesel Allison; NASA Contract DEN3-17.) NASA CR-159865, 1980.
2. Fisher, E. A. and Trela, W.: The Evaluation of Ceramic Turbine Stators. Presented at the 6th U.S. Army Materials Technology Conference, Orcas Island, Washington, July 10-13, 1979.
3. Bratton, R. J.; Holden, A. N.; and Mumford, S. E.: Testing Ceramic Stator Vanes for Industrial Gas Turbines. SAE paper 740236, Feb. 1974.
4. Kennedy, F. E.; and Bill, R. C.: Thermal Stress Analysis of Ceramic Gas-Path Seal Components for Aircraft Turbines. NASA TP-1437, 1979.
5. Bill, R. C.; Wisander, D. W.; and Brewe, D. E.: Preliminary Study of Methods Providing Thermal Shock Resistance to Plasma-Sprayed Ceramics Gas-Path Seals. NASA TP-1561, 1980.
6. Ludwig, Lawrence P.: Gas Turbine Engine with Fuel Cooled Turbine Disk. NASA Case No. 13,325-1, Apr. 13, 1979.
7. Liebert, C. H.; and Gaugler, R. E.: Significance of Thermal Contact Resistance in Two-Layer Thermal-Barrier-Coated Turbine Vanes. NASA TM-81483, 1980.
8. Wong, K. F.; and Dybbs, A.: An Experimental Study of Thermal Equilibrium in Liquid Saturated Porous Media. Int. J. Heat Mass Transfer, vol. 19, no. 2, Feb. 1976, pp. 234-236.
9. Stepka, Francis S.: Thermal and Flow Analysis of a Convection Air-Cooled Ceramic Coated Porous Metal Concept for Turbine Vanes. NASA TM-81749, 1981.
10. Gauntner, D. J.; and Sucec, J.: Method for Calculating Convective Heat Transfer Coefficients Over Turbine Vane Surfaces. NASA TP-1134, 1978.
11. Carmen, P. C.: Flow of Gases Through Porous Media. Butterworths Scientific Publications (London), 1956.
12. Shiembob, L. T.: Development of a Plasma Sprayed Ceramic Gas Path Seal for High Pressure Turbine Applications. (PWA-5569-12, Pratt & Whitney Aircraft Group; NASA Contract NAS3-20623.) NASA CR-135387, 1978.

1. Report No. NASA TP-1942 AVRADCOM TR 81-C-7		2. Government Accession No.		3. Recipient's Catalog No.	
4. Title and Subtitle GAS TURBINE CERAMIC-COATED-VANE CONCEPT WITH CONVECTION-COOLED POROUS METAL CORE				5. Report Date December 1981	
				6. Performing Organization Code 307-90-00	
7. Author(s) Albert F. Kascak, Curt H. Liebert, Robert F. Handschuh, and Lawrence P. Ludwig				8. Performing Organization Report No. E-732	
				10. Work Unit No.	
9. Performing Organization Name and Address NASA Lewis Research Center and Propulsion Laboratory AVRADCOM Research and Technology Laboratories Cleveland, OH 44135				11. Contract or Grant No.	
				13. Type of Report and Period Covered Technical Paper	
12. Sponsoring Agency Name and Address National Aeronautics and Space Administration Washington, DC 20546 and U.S. Army Aviation Research and Development Command St. Louis, MO 63166				14. Sponsoring Agency Code	
15. Supplementary Notes Albert F. Kascak: Propulsion Laboratory, AVRADCOM Research and Technology Laboratories. Curt H. Liebert, Robert F. Handschuh, and Lawrence P. Ludwig: Lewis Research Center.					
16. Abstract Analysis and flow experiments on a ceramic-coated-porous-metal vane concept indicated the feasibility, from a heat transfer standpoint, of operating in a high-temperature (1644 K; 2500° F) gas turbine cascade facility. The heat transfer and pressure drop calculations provided a basis for selecting the ceramic layer thickness (to 2.03 mm; 0.08 in.), which was found to be the dominant factor in the overall heat transfer coefficient. Also an approximate analysis of the heat transfer in the vane trailing edge revealed that with trailing-edge ejection the ceramic thickness could be reduced to 0.254 mm (0.01 in.) in this portion of the vane.					
17. Key Words (Suggested by Author(s)) Ceramic-coated turbine vanes			18. Distribution Statement Unclassified - unlimited STAR Category 07		
19. Security Classif. (of this report) Unclassified		20. Security Classif. (of this page) Unclassified		21. No. of Pages 13	
				22. Price* A02	

* For sale by the National Technical Information Service, Springfield, Virginia 22161

National Aeronautics and
Space Administration

Washington, D.C.
20546

Official Business

Penalty for Private Use, \$300

SPECIAL FOURTH CLASS MAIL
BOOK

Postage and Fees Paid
National Aeronautics and
Space Administration
NASA-451



4 1 10, A, 120351 80090305
DEPT OF THE AIR FORCE
AF WEAPONS LABORATORY
ATTN: TECHNICAL LIBRARY (SOL)
CIRLEAD AFB WA 97117

NASA

POSTMASTER:

If Undeliverable (Section 158
Postal Manual) Do Not Return